

Physico-chemical Processes Occurring Inside a Pyrolyzing Two-Dimensional Tobacco Particle

Sung Chul Yi[†]

Department of Chemical Engineering, CPRC, Hanyang University, Seoul 133-791, Korea

(Received 3 October 2002 • accepted 27 November 2002)

Abstract—A two-dimensional, variable property, mathematical model of the transient pyrolysis of tobacco particle, in response to the smoldering (low heating rate) and puffing (fast heating rate) conditions in a burning cigarette, is presented. The model considers pyrolysis of tobacco obeying four-step Arrhenius kinetics, evaporation of water from tobacco following a mass-transfer and rate-determined process, and the formation of carbonaceous residue. From the physical point of view, the model describes convective, conductive and radiative heat transfer, and velocity and pressure variations interior to the porous tobacco particle (Darcy's law). Furthermore, porosity, permeability and thermal conductivity vary with the composition of the reacting medium. Time and space evolution of the main variables, and reaction product distribution, are simulated by varying the tobacco heating rates.

Key words: Tobacco Pyrolysis, Mathematical Model, Smoldering, Puffing

INTRODUCTION

Tobacco pyrolysis is a problem of interest in the field of the generation of the smoke constituents. The burning behavior of tobacco is characterized by two distinct processes - an exothermic combustion and an endothermic pyrolysis/distillation. Most of the gas and particulate phase smoke may be generated in the pyrolysis zone. The major gas phase products in the oxygen deficient pyrolysis zone [Baker et al., 1973] are CO and CO₂. This is typical for cellulosic materials. Pyrolysis is a fundamental step in a burning cigarette, following solid drying and preceding char combustion. Pyrolysis is a complex process dominated by a strong interaction between transport phenomena and chemical reactions.

Basic process characteristics have been investigated with respect to the pyrolysis of individual compounds found in tobacco, extracts from tobacco, and tobacco itself. The main objectives for the experiments were from trying to develop tools to predict the smoke yield and to the mapping of thermal decomposition pathways and classic precursor/product studies. Researchers have tried to mimic pyrolysis methods more like the conditions in a burning cigarette. From simply heating a sample in the furnace to sophisticated equipment that attempts to match the conditions in a cigarette have been developed. Smith et al. [1975] and Higman et al. [1977] have built pulsed systems that move a furnace along a tube containing the tobacco. The gas flow could also be pulsed to simulate a puff. In spite of the numerous experimental efforts, most researchers realize that the results from the pyrolysis experiments cannot be used to reliably determine the processes that occur in a burning cigarette.

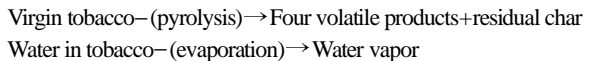
The modeling literature on the pyrolysis of the tobacco has been reviewed by Baker et al. [1990]. In the meanwhile, Yi et al. [2002] have proposed the comprehensive single particle model where multi-

step pyrolysis schemes, including one-stage, multi-reactions of primary pyrolysis process, have been coupled to the description of the main physical processes. Mathematical models of pyrolysis process inside a burning cigarette have been published to predict the temperature and pyrolysis products distributions [Yi et al., 2001, Muramatsu et al., 1979].

In this work, a two-dimensional, unsteady model of a single particle pyrolysis is presented to explain an adequate description of the anisotropic flow of pyrolysis products and to quantify its implication in the pyrolytic degradation. The influence of heat transfer mechanisms is investigated on the structure of the pyrolysis front and global pyrolysis characteristics.

MATHEMATICAL FORMULATION OF THE PROBLEM

To describe the primary reactions of tobacco pyrolysis, the one-step global model is based on the lumping of the different products into five groups: residual char, four volatile products, as well as water in tobacco into water vapor by evaporation. The kinetic data by Muramatsu et al. [1979] was used to model primary degradation of the tobacco particle:



From the physical point of view, the model here presented describes the transport phenomena occurring through the cross-section of a tobacco particle exposed in a burning cigarette. In a burning cigarette, the thermal structure of a burning zone is dynamic, with heating rates that vary dramatically from 15 K/s during smoldering to 500 K/s during puffing. Because of such complexity, it is extremely difficult to determine the rates of reactions, and mechanisms of formation of individual smoke constituents and their yields. Due to the symmetry of the problem, one-fourth of the tobacco particle is considered, according to the schematic reported in Fig. 1. Initial and boundary conditions of the model are also included.

[†]To whom correspondence should be addressed.

E-mail: scyi@email.hanyang.ac.kr

[‡]This paper is dedicated to Professor Baik-Hyon Ha on the occasion of his retirement from Hanyang University.

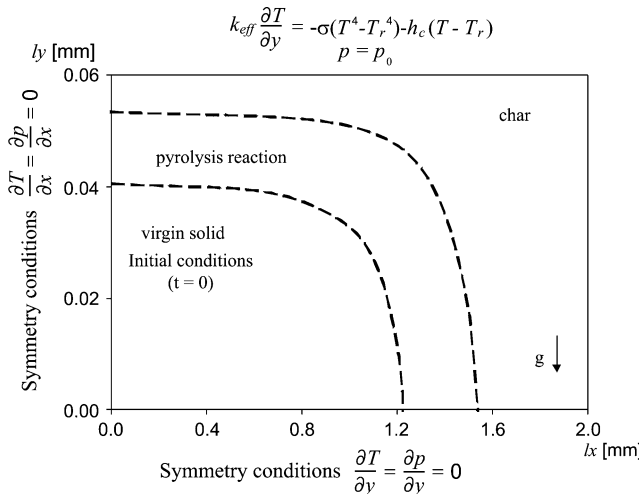


Fig. 1. Schematic of tobacco pyrolysis.

The formulation of the mathematical model is based on the assumptions of no thermal swelling and/or shrinkage and surface regression as the tobacco undergoes pyrolysis, local thermal equilibrium between the solid and the volatile products, and no condensation of water. Physical processes described include the radiative, convective and conductive heat transfer interior to the particle from the exposed surfaces, momentum transfer to account for non zero pressure gradients and non uniform velocity, variable properties (thermal conductivity, porosity and permeability vary linearly with the conversion), accumulation of the volatile energy mass and the volatile transport through the virgin tobacco and the charred region.

1. Transport Phenomena in the Tobacco

Transport phenomena in the tobacco particle include heat conduction upon heating, convection due to gas and volatile generation, and radiation. The pressure and velocity variations in the particle can be described by Darcy's law. As chemical reactions occur, properties such as porosity, effective thermal conductivity, permeability and gas and solid volume change. Energy conservation can be expressed in terms of total enthalpy, which includes accumulation of enthalpy of tobacco and gas-phase-species, the convective transport of gas-phase species, the conductive transport of heat and the heat release associated with chemical reactions

$$\begin{aligned} \frac{\partial}{\partial t}(\rho_v h_v + \rho_c h_c + \rho_w h_w + \epsilon \rho_g h_{gas}) + \frac{\partial}{\partial x}(\rho_s h_s u) + \frac{\partial}{\partial y}(\rho_s h_s v) \\ = \frac{\partial}{\partial x}\left(k_{eff} \frac{\partial T}{\partial x}\right) + \frac{\partial}{\partial y}\left(k_{eff} \frac{\partial T}{\partial y}\right) + \frac{\partial \rho_w}{\partial t} \Delta H_w \end{aligned} \quad (1)$$

By means of specific enthalpies of chemical species defined as

$$h_v = c_{pv} T, h_c = c_{pc} T, h_w = c_{pw} T, h_g = c_{pg} T$$

the energy balance equation becomes:

$$\begin{aligned} \frac{\partial}{\partial t}\{(\rho_v c_{pv} + \rho_c c_{pc} + \rho_w c_{pw} + \epsilon \rho_g c_{pg})T\} + \frac{\partial}{\partial x}(\rho_s c_{pg} u T) \\ + \frac{\partial}{\partial y}(\rho_s c_{pg} v T) = \frac{\partial}{\partial x}\left(k_{eff} \frac{\partial T}{\partial x}\right) + \frac{\partial}{\partial y}\left(k_{eff} \frac{\partial T}{\partial y}\right) + \frac{\partial \rho_w}{\partial t} \Delta H_w \end{aligned} \quad (2)$$

The effective thermal conductivity consists of both conduction and radiation contributions and may be expressed as:

$$\begin{aligned} k_{eff} &= k_{con} + k_{rad} \\ k_{con} &= \eta k_v + (1-\eta) k_c + \phi k_g \\ k_{rad} &= \sigma T^3 d/\omega \end{aligned} \quad (3)$$

The conservation equation for the total gas-phase species can be considered:

$$\frac{\partial(\epsilon \rho_g)}{\partial t} + \frac{\partial}{\partial x}(\rho_g u) + \frac{\partial}{\partial y}(\rho_g v) = \Omega_g \quad (4)$$

$$\text{where, } \Omega_g = -\left(1 - \frac{\rho_f}{\rho_{v0}}\right) \frac{\partial \rho_v}{\partial t} - \frac{\partial \rho_w}{\partial t}$$

Momentum transfer will be described according to Darcy's law:

$$u = -\frac{K \partial p}{\mu \partial x}, v = -\frac{K}{\mu} \left(\frac{\partial p}{\partial y} + \rho_g g \right) \quad (5)$$

The permeability in Darcy's law varies with the composition according to a linear dependence:

$$K = \eta K_v + (1-\eta) K_c \quad (6)$$

$$\text{where, } \eta = \frac{\rho_v}{\rho_{v0}}$$

The mixture of gases inside the porous solid behaves according to the ideal gas law:

$$\rho_g = \frac{PM_g}{RT} \quad (7)$$

Finally, we substitute the total continuity equation with a pressure evolution equation, obtained through a combination of total continuity, equation of state and momentum equations:

$$\frac{\partial(\epsilon p/T)}{\partial t} = \frac{\partial}{\partial x}\left(\frac{K p \partial p}{\mu T \partial x}\right) + \frac{\partial}{\partial y}\left(\frac{K p \partial p}{\mu T \partial y}\right) + \frac{M_g}{R} \frac{\partial}{\partial y}\left(\frac{K p^2 g}{\mu T^2}\right) + \frac{R}{M_g} \Omega_g \quad (8)$$

2. Water Evaporation

As the temperature of the tobacco particles increases, the water content in the tobacco evaporates. A detailed description of the formulation of the water evaporation can be found from the work done by Muramatsu et al. [1979].

The evaporation rate of water from tobacco can be expressed by the empirical equation:

$$\frac{\partial \rho_w}{\partial t} = -N_a \alpha \exp\left(-\frac{\theta}{T}\right) (w - w_{eq})^\beta = \sum_{i=1}^4 \rho_{v,i}^0 \frac{\partial w}{\partial t} \quad (9)$$

where N_a is total surface area of tobacco shreds per unit volume of a cigarette, θ is experimental constant, and w_{eq} is related to the water vapor pressure, p_w , by:

$$w_{eq} = \frac{p_w/p_{ws}}{a + b(p_w/p_{ws}) - c(p_w/p_{ws})^2}$$

The saturated vapor pressure of water, p_{ws} , can be expressed by Collingaert's equation as follows:

$$\log p_{ws} = 7.991 - \frac{1687}{T-43}$$

Water vapor pressure inside the particle is given by the following mass-balance equation:

$$\frac{\partial}{\partial t}\left(\frac{p_w}{RT}\right) + \frac{\partial}{\partial x}\left(u \frac{p_w}{RT}\right) + \frac{\partial}{\partial y}\left(v \frac{p_w}{RT}\right)$$

$$= \frac{\partial}{\partial x} \left\{ D_{eff} \frac{\partial}{\partial x} \left(\frac{p_w}{RT} \right) \right\} + \frac{\partial}{\partial y} \left\{ D_{eff} \frac{\partial}{\partial y} \left(\frac{p_w}{RT} \right) \right\} - \frac{R}{M_w} \frac{\partial p_w}{\partial t} \quad (10)$$

The kinetic data and associated parameters of Muramatsu et al. [1979] were used.

3. Tobacco Pyrolysis

Followed by water evaporation, the virgin tobacco is gradually consumed by pyrolysis. The changes in density of the virgin tobacco by pyrolysis were represented by an n^th order Arrhenius equation. The rate of pyrolysis of tobacco is equal to the sum of four different pyrolysis reactions. The rate of increase in the density of the carbonaceous residue can also be predicted from the pyrolysis rate. The kinetic data and associated parameters were taken from a paper by Muramatsu et al. [1979].

The conversion of virgin tobacco can be represented by the following four reactions:

$$\frac{\partial \rho_v}{\partial t} = \sum_{i=1}^4 \frac{\partial \rho_{v,i}}{\partial t} \quad (11)$$

$$\frac{\partial \rho_{v,i}}{\partial t} = -A_i \exp\left(-\frac{E_i}{RT}\right) \left(\frac{\rho_{v,i}}{\rho_{v,i}^0}\right)^{n_i} \rho_{v,i}^0 \text{ where, } i=1\Lambda 4 \quad (12)$$

The residual char density is given by:

$$\frac{\partial \rho_c}{\partial t} = - \frac{\rho_f}{\sum_{i=1}^4 \rho_{v,i}^0} \frac{\partial \rho_v}{\partial t} \quad (13)$$

where superscript 0 is the initial state.

The equation describing time evolution of solid volume, V_s , is written assuming that

$$\frac{V_s}{V_{s0}} = \frac{m_v + m_c + m_w}{m_{s0}} = \frac{\rho_v + \rho_c + \rho_w}{\rho_{s0}} \quad (14)$$

and the porosity of the medium is given by $\epsilon = \frac{V_s}{V}$

The above relation for porosity can be rewritten as follows under the assumption that the total volume occupied by the tobacco particle does not change as the solid undergoes pyrolysis:

$$\epsilon = 1 - \frac{V_s}{V} = 1 - \frac{V_{s0}}{V} \left(\frac{\rho_v + \rho_c + \rho_w}{\rho_{s0}} \right) \quad (15)$$

Therefore, temporal change of porosity of tobacco particle can be written as:

$$\frac{\partial \epsilon}{\partial t} = - \frac{V_{s0}}{V \rho_{s0}} \left(\frac{\partial \rho_v}{\partial t} + \frac{\partial \rho_w}{\partial t} + \frac{\partial \rho_c}{\partial t} \right) \quad (16)$$

4. Initial and Boundary Conditions

Initially, the tobacco particle is at ambient condition and is suddenly exposed in an inert atmosphere, where the pressure is p_0 and the temperature is T_r . At the top and right surfaces, it impermeable to mass flow, and adiabatic conditions to others are assigned.

$$x=lx: k_{eff} \frac{\partial T}{\partial x} = -\epsilon_r \sigma (T^4 - T_r^4) - h_c (T - T_r), \quad p=p_0 \quad (17)$$

$$y=ly: k_{eff} \frac{\partial T}{\partial y} = -\epsilon_r \sigma (T^4 - T_r^4) - h_c (T - T_r), \quad p=p_0 \quad (18)$$

(at the other two sides, $x=0$, and $y=0$, symmetry conditions are im-

posed).

The model Eqs. (1)-(12) with initial and boundary conditions are implemented in commercially available computational fluid dynamics code, FLUENT, using user-defined-functions (UDFs).

MODEL IMPLEMENTATION

The implementation of the models described above is done in a commercial computational fluid dynamics (CFD) code, Fluent 6.0. All equations are solved sequentially and iteratively in keeping with the Fluent algorithms. Most of the processes occurring inside the tobacco shred cannot be simulated by using the standard version of Fluent software. Therefore, the equations described above are incorporated through the user-defined-functions (UDFs) available in Fluent by solving new sets of scalar equations. A brief description of the udfs developed in this work is given below.

Description of "PYROLYSIS.h"

There are a total of three user-defined-scalar (UDS) and seven user-defined-memory variables (UDMs) defined in this problem. In the header file "PYROLYSIS.h" all the parameters required for setting up the problem are given as inputs. The variable names and comment lines together give details of the units of different inputs.

Description of "PYROLYSIS.c"

The function DEFINE_INIT (initialize_function, domain) is used for initializing all the user-defined-memory variables. This function is called when the problem is initialized in FLUENT.

The function DEFINE_ADJUST (adjust_function, domain) is written for calculating temperature, total pressure and water vapor pressure during transient calculations. This function is called before each iteration. The comment statements before different pieces of this function explain what each part is doing.

The function DEFINE_SOURCE (energy_source, c, t, dS, eqn) sets the source/sink term in the energy balance equation.

The function DEFINE_UDS_UNSTEADY (UDS_unsteady_condition, c, t, i, apu, su) sets transient terms for user-defined scalars, UDS-0-UDS-2 and user-defined-memories, UDM-0-UDM-7.

The function DEFINE_DIFFUSIVITY (UDS_diffusion_coeff, c, t, i) computes diffusivity value to be used in the user-defined-scalar equations.

The function DEFINE_PROFILE (convective_bc_UDS_0, thread, i) is used for setting flux boundary condition on different boundaries.

RESULTS AND DISCUSSION

The properties used in the numerical simulations describe a tobacco pyrolysis. The kinetic data and the tobacco particle properties are the same as in Muramatsu et al. [1979]. Effective thermal conductivity is taken from Blasi [1996] and permeabilities are estimated so as to provide gas overpressures of the same order as those experimentally observed for the cellulosic samples [Lee et al., 1976]. Simulations have been made for anisotropic particles of $lx=30$ mm and $ly=0.06$ mm. A two-dimensional computational mesh of 1800 quadrilateral cells is created for the analysis.

The simulations are made from room temperature, with a fixed final temperature. The product yield of single tobacco shred is predicted, using a low heating rate of 15 K/s for smoldering [Mur-

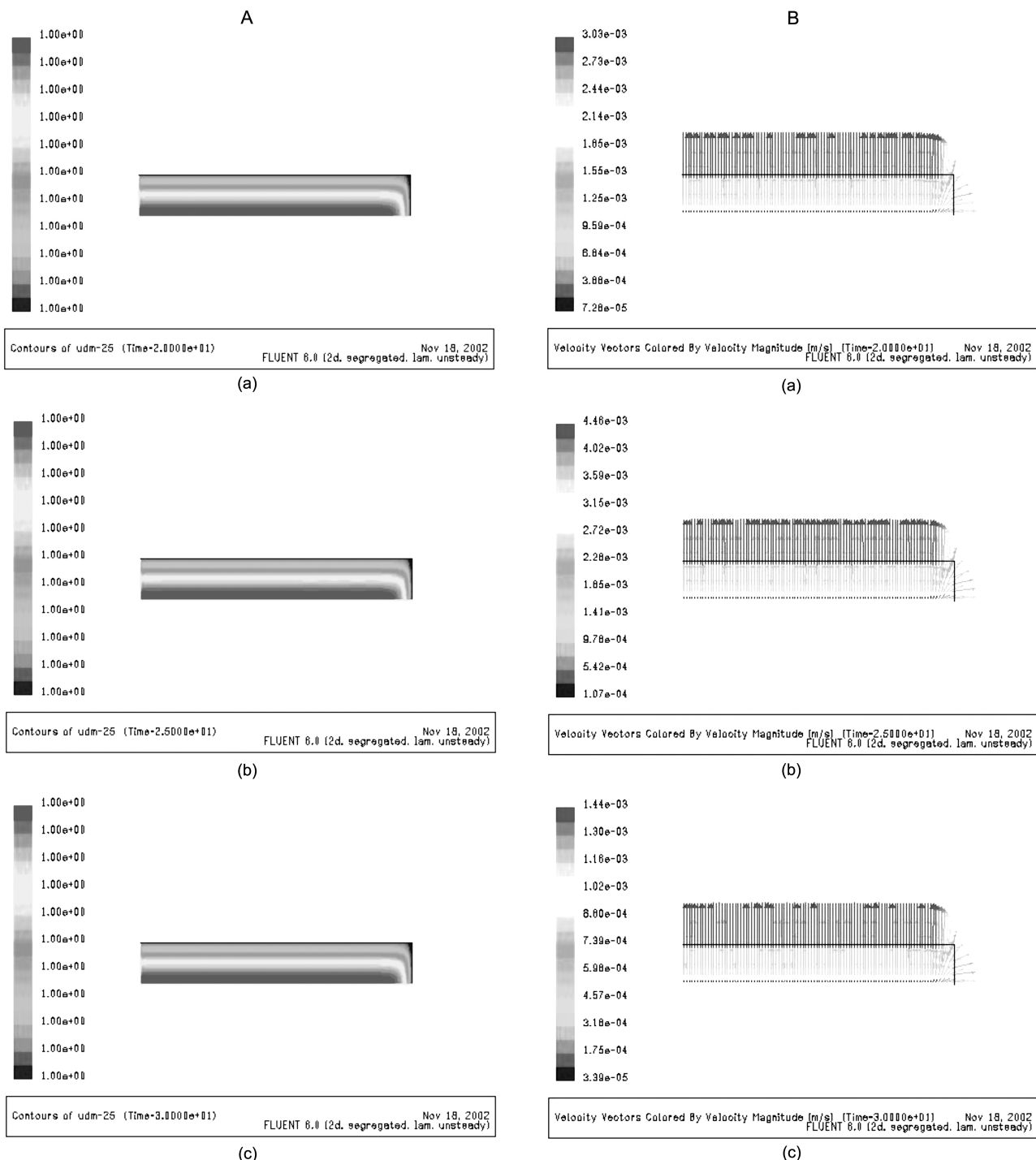


Fig. 2. A. Contours of gas overpressure from 101325 Pa for (heating rate=15 K/s) (a) 20.0 sec, (b) 25.0 sec, and (c) 30.0 sec smoldering (y-axis enlarged by 5 times). B. Contours of velocity vector field for smoldering (heating rate=15 K/s) (a) 20.0 sec, (b) 25.0 sec, and (c) 30.0 sec smoldering (y-axis enlarged by 5 times).

matsu et al., 1979], a high heating rate of 500 K/s for puffing [Baker, 1975] and a final pyrolysis temperature of 450 °C.

Temporal and spatial evolution of the pyrolysis process is shown through distributions of gas overpressure from 101325 Pa and velocity vector fields in Figs. 2A to 2B at several times for the smoldering and puffing.

Volatile species generated in the pyrolysis region create a con-

vective transport which is affected by the structure of the solid residue. Clearly, pressure gradients are establishing along the tobacco shred for smoldering and puffing in Figs. 3A and 3B. The velocity characterizing the mass flow of volatile species is the result of the net reaction production and pressure variations. Velocity increases with time since the pyrolysis occurs on the whole tobacco shred. After reaching its maximum, velocity decreases since the amount

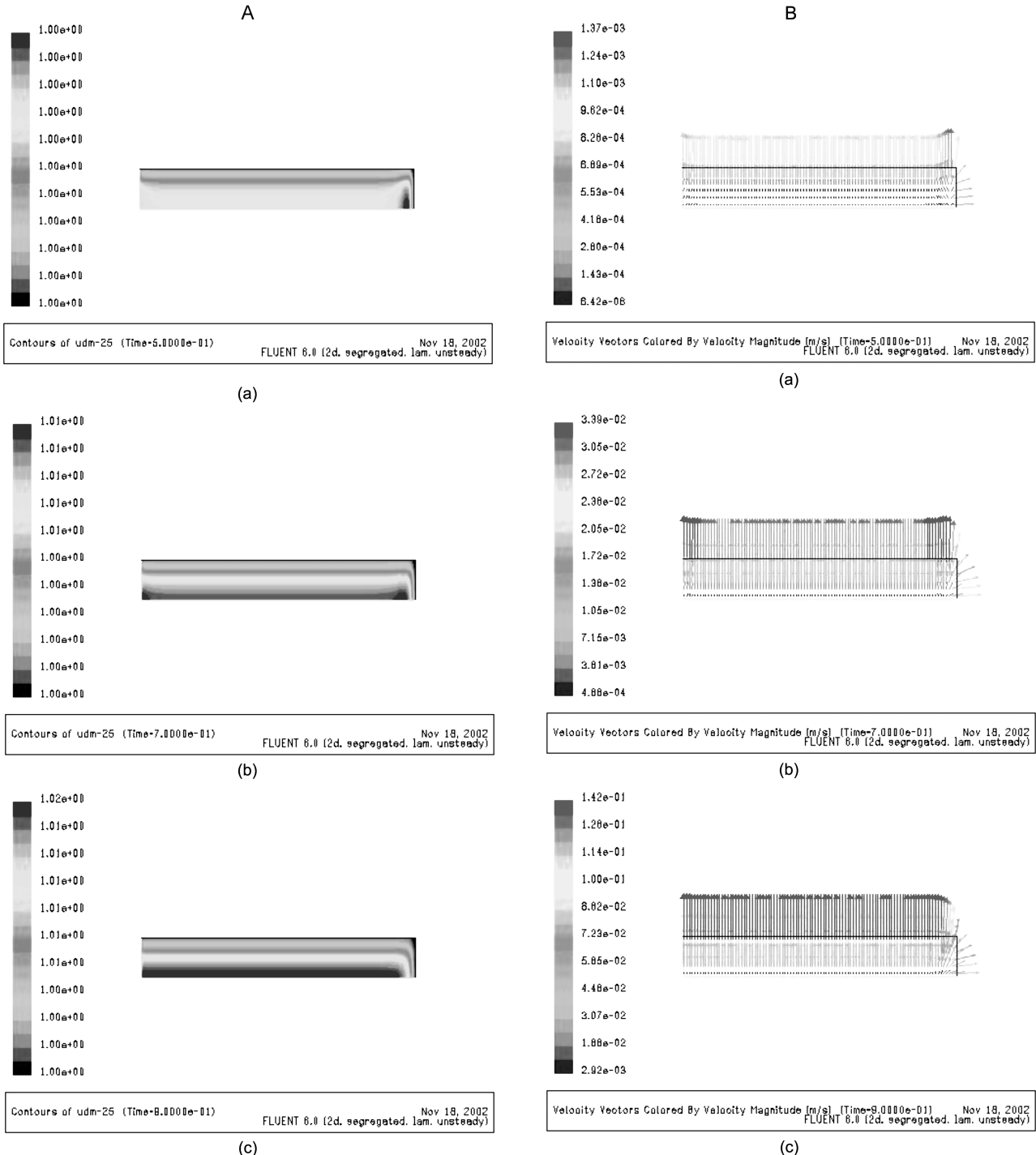


Fig. 3. A. Contours of gas overpressure from 101325 Pa for puffing (heating rate=500.0 K/s) (a) 0.5 sec, (b) 0.7 sec, and (c) 0.9 sec (y-axis enlarged by 5 times). B. Contours of velocity vector field for puffing (heating rate=500.0 K/s) (a) 0.5 sec, (b) 0.7 sec, and (c) 0.9 sec (y-axis enlarged by 5 times).

of volatile species in the tobacco shred decreases leading to the lower pressure inside. As expected, the overpressure and velocity in the shred for puffing are much larger than those for smoldering due to the much shorter reaction time.

The simulated dynamics of the area-weighted average gas overpressure and velocity are shown in Figs. 4A and 4B for smoldering and puffing. As reported by Muramatsu et al. [1979] and Val-

verde et al. [2000], volatiles in tobacco could be divided into multiple noninteracting mass-loss events clearly shown in Fig. 4A.

Spatial temperature gradients for smoldering and puffing are shown in Figs. 5A and 5B at the pyrolysis temperature. As shown in Fig. 5A, temperature gradients for smoldering are practically negligible due to the thickness of the tobacco shred and the heating rate. Similar results are reported in the study of cellulose pyrolysis by

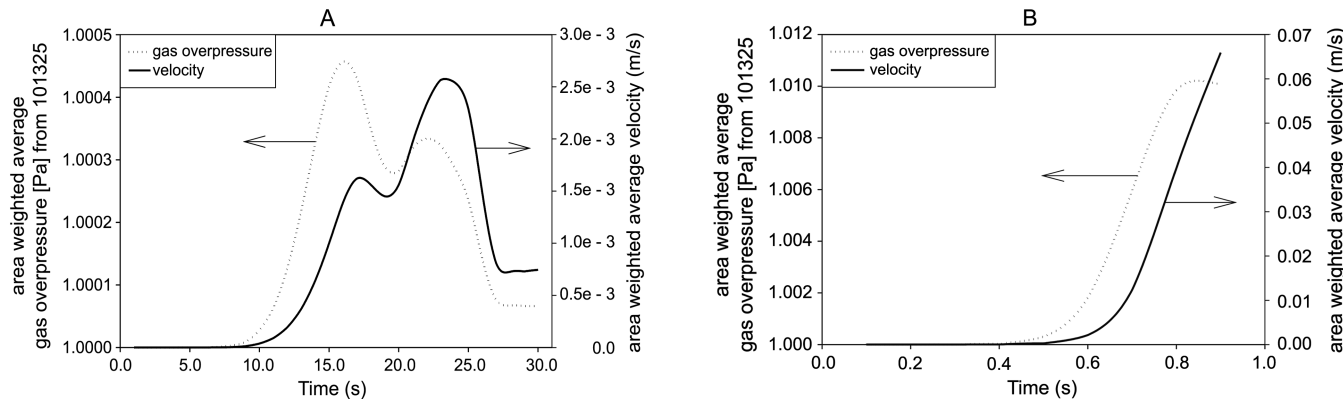


Fig. 4. A. Dynamics of area weighted gas overpressure and velocity for smoldering (heating rate=15.0 K/s, $T_{pyro}=723.0$ K). B. Dynamics of area weighted gas overpressure and velocity for puffing (heating rate=500.0 K/s, $T_{pyro}=723.0$ K).

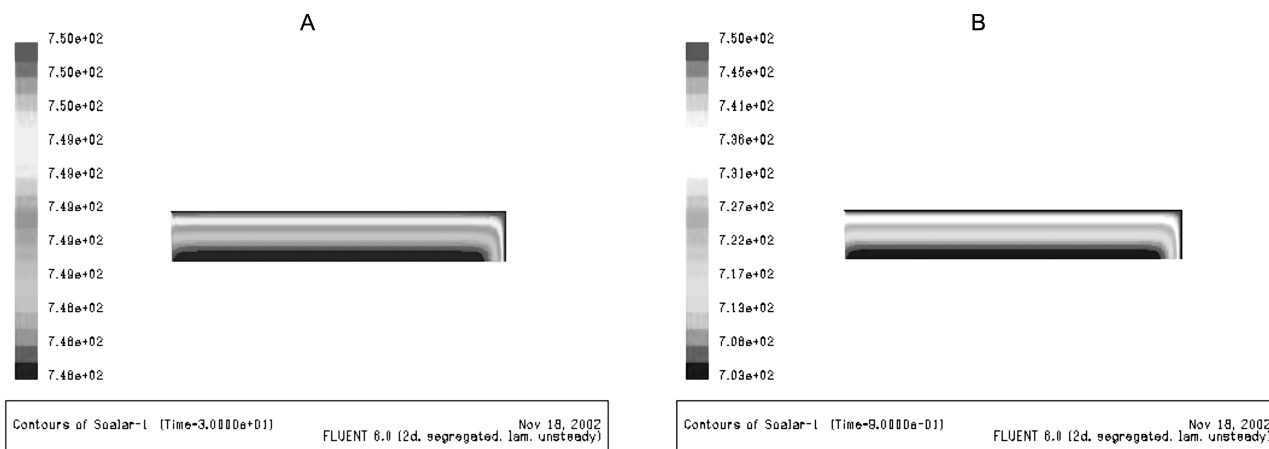


Fig. 5. A. Contours of temperature for smoldering (heating rate=15.0 K/s, $T_{pyro}=723.0$ K) (y-axis enlarged by 5 times). B. Contours of temperature for puffing (heating rate=500.0 K/s, $T_{pyro}=723.0$ K) (y-axis enlarged by 5 times).

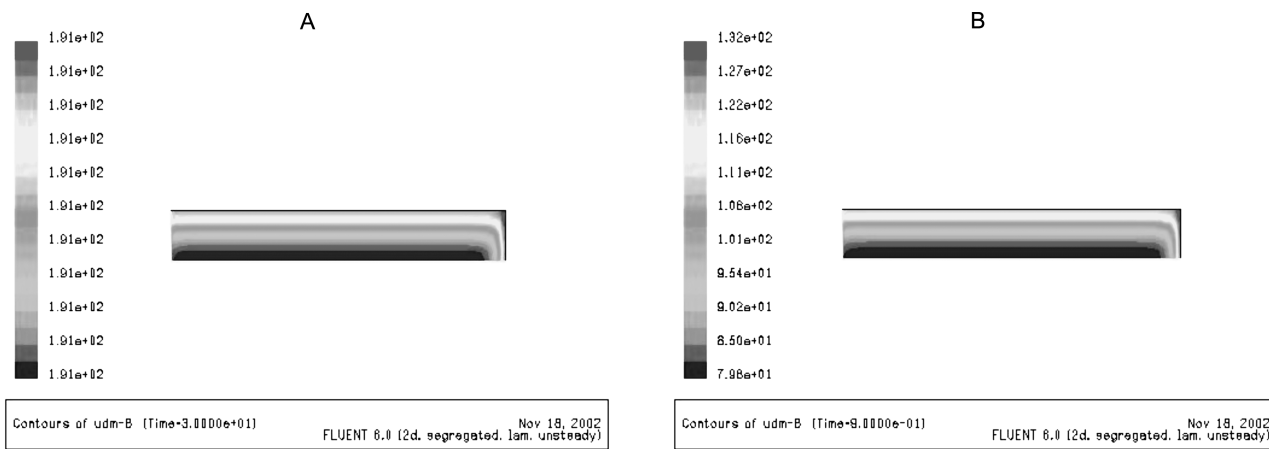


Fig. 6. A. Contours of char concentration for smoldering (heating rate=15.0 K/s, $T_{pyro}=723.0$ K) (y-axis enlarged by 5 times). B. Contours of char concentration for puffing (heating rate=500.0 K/s, $T_{pyro}=723.0$ K) (y-axis enlarged by 5 times).

Blasi [1996]. In her study the thickness of 200 μm is the critical value for thermally thin regime and 10 μm is assumed to be the limit of pure kinetic control.

Figs. 6A and 6B show the final char yield, for smoldering and puffing conditions, on the final pyrolysis temperature. Larger char concentration gradients are observed for puffing, high heating con-

dition due to the larger temperature gradients, which could lead to the more diverse of combustion products for puffing condition.

CONCLUSIONS

A two-dimensional, unsteady model has been developed to sim-

ulate the pyrolysis of a single tobacco particle. The large uncertainty about the parameters on tobacco pyrolysis makes any qualitative comparison between predictions and experimental results difficult. However, qualitative agreement is obtained and the model predictions shed light on the physical mechanisms affecting the tobacco pyrolysis for smoldering and puffing conditions. The pyrolysis process for smoldering has been identified as thermally thin regime where intraparticle temperature is uniform, though this may continue to change, depending on external conditions.

Further improvements in the mathematical model of tobacco pyrolysis should include the detailed kinetics of the pyrolysis products and the secondary reactions whose extent is influenced by both reaction temperature and the volatile residence time as well as the physical properties of the tobacco particle.

ACKNOWLEDGEMENT

This research is supported in part by Ceramic Processing Research Center (CPRC) and the author gratefully appreciates the financial support.

NOMENCLATURE

A	: pre-exponential factor
c_p	: specific heat
D	: diffusivity
d	: pore diameter
E	: activation energy
g	: gravitational acceleration
h	: specific enthalphy per unit mass
h_c	: convective heat transfer coefficient
k	: thermal conductivity
lx	: x-direction length
ly	: y-direction length
M	: molecular weight
N_a	: total surface area of tobacco shreds per unit volume
p	: pressure
R	: universal constant
T	: temperature
t	: time
V	: volume
w	: water content

Greek Letters

ΔH	: heat of reaction
ϵ	: porosity
ϵ_i	: emissivity
η	: ratio between char and virgin material
κ	: permeability
μ	: viscosity
ρ	: mass concentration
σ	: Stefan-Boltzmann constant

ϕ	: total void fraction based on real density
ω	: radiative emissivity

Subscripts

c	: char
con	: conductive mode
eff	: effective
eq	: equilibrium
f	: final state
g	: gas phase
i	: i species
r	: surrounding state
rad	: radiative mode
s	: virgin solid
v	: virgin tobacco
w	: water
ws	: saturated water
0	: initial state

REFERENCES

Baker, R. R. and Kilburn, K. D., "The Distribution of Gases Within the Combustion Coal of a Cigarette," *Beitr. Tabakforsch.*, **7**, 79 (1973).

Baker, R. R. and Robinson, D. P., "Tobacco Combustion- the Last Ten Years," *Rec. Adv. Tob. Sci.*, **16**, 3 (1990).

Baker, R. R., "Temperature Variation Within a Cigarette Combustion Coal During the Smoking Cycle," *High Temperature Science*, **7**, 236 (1975).

Blasi, C. D., "Kinetic and Heat Transfer Control in the Slow and Flash Pyrolysis of Solids," *Ind. Eng. Chem. Res.*, **35**, 37 (1996).

Higman, E. B., Severson, R. F., Arrendale, R. F. and Chortyk, O. T., "Simulation of Smoking Conditions by Pyrolysis," *J. Agri. Food Chem.*, **25**, 1201 (1977).

Lee, C. K., Chaiken, R. F. and Singer, J. M., "Charring Pyrolysis of Wood in Fires by Kaser Simulation," Sixteenth Symposium (Int.) on Combustion, *The Combustion Institute*, 1459 (1976).

Muramatsu, M., Umemura, S. and Okada, T., "A Mathematical Model of Evaporation Processes Inside a Naturally Smoldering Cigarette," *Combust. Flame*, **36**, 245 (1979).

Smith, W. T. Jr., Chen, S. P. and Patterson, J. M., "Effect of Some Pyrolytic Parameters on Cyanide Production During the Controlled Pyrolysis of Tobacco," *Tob. Sci.*, **19**, 50 (1975).

Valverde, J. L., Curbelo, C., Mayo, O. and Molina, C. B., "Pyrolysis Kinetics of Tobacco Dust," *Trans IChemE*, **78**, 921 (2000).

Yi, S. C. and Hajaligol, M. R., "Product Distribution from the Pyrolysis Modeling of Tobacco Particles," *J. of Analytical and Applied Pyrolysis*, accepted for the publication (2002).

Yi, S. C., Song, E. S. and Hajaligol, M. R., "Mathematical Model of Smoldering Combustion in a Carbonaceous Porous Medium Part 1- Development of Pyrolysis and Combustion Models for a Cylindrical Geometry," *J of Fire Sciences*, **19**, 429 (2001).